ORIGINAL PAPER

Diurnal variation in the occurrence frequency of the Tibetan Plateau vortices

Lun Li · Renhe Zhang · Min Wen

Abstract A diagnostic study is made on the diurnal variation in the occurrence frequency of the Tibetan Plateau vortices (TPVs) in four local time (LT) periods of a day (06–12 LT, 12–18 LT, 18–00 LT, 00–06 LT) using the data from May to September in 2006–2008. The occurrence frequency of the TPVs shows a robust diurnal variation with its maximum from evening to midnight (18–00 LT) and minimum from early morning to noon (06–12 LT). The physical processes in association with the diurnal variation of the TPVs are revealed. Both large-scale circulations and condensational latent heat induced by the precipitation system have important effect on the diurnal variation of the TPVs' occurrence. In the evening at 18 LT, there are strongest convergence at 500 hPa and divergence at 200 hPa. Meanwhile, the largest water vapor is transported to the main body of the Tibetan Plateau, and the stratification is unstable, which are conducive to the strongest convection and condensational latent heat release accompanied with the largest precipitation system. All these conditions are responsible for the maximum occurrence of the TPVs in 18–00 LT. On the contrary, at 06 LT the weakest convergence at 500 hPa and divergence at 200 hPa as well as the stable stratification result in little latent heat release, and the minimum occurrence of the TPVs is observed in 06–12 LT.

L. Li · R. Zhang (✉) · M. Wen
State Key Laboratory of Severe Weather, Chinese Academy of Meteorological Sciences, 46 Zhong-Guan-Cun South Avenue, Beijing 100081, China
e-mail: renhe@cams.cma.gov.cn

1 Introduction

The Tibetan Plateau vortices (TPVs) are of specific synoptic system over the Tibetan Plateau in boreal summer, with typical spatial scales of 400–800 km in horizontal and 2–3 km in vertical, respectively (Ye and Gao 1979; Luo 1992). The previous studies showed that the TPVs mainly form over the central-western plateau in the period from June to August, and much less in May and September; the peak of occurrence frequency of the vortices appears in June; and most of the TPVs die out in situ in 12–24 h, some can develop and move eastward with a few moving off the Tibetan Plateau (Ye and Gao 1979; Luo 1992; Qiao and Zhang 1994; Chen et al. 1996). The TPVs not only have important effect on the precipitation over the main body of the Tibetan Plateau, but also are closely related to the rainfall to the east of the Tibetan Plateau in southwestern and eastern China. Several heavy floods over the middle and lower reaches of the Yangtze River valley and over the Huaihe River basin are triggered by the TPVs moving off the Tibetan Plateau (Tao and Ding 1981; Yang et al. 2001; Yi and Xu 2001; Li 2002; Yu 2008). Therefore, the research on the activities of the TPVs has great significance in understanding the severe weather not only over the Tibetan Plateau, but also over the regions to the east of the Tibetan Plateau.

The generation and evolution mechanisms of the TPVs have been investigated by many researchers. For the generation process of the TPVs, some studies stressed that the condensational latent heat release plays dominant role (Dell'Osso and Chen 1986; Wang 1987; Li et al. 2011), while some others pointed out that the sensible heating is a major factor (LG-TPMR[1] 1981; Shen et al. 1986b; Li and Zhao

---

[1] LG-TPMR stands for Lhasa Group for Tibetan Plateau Meteorology Research.

2002), and the dynamic effect is less important (Chen et al. 1996). After the vortices are formed, the condensational latent heat exerts a remarkable effect on the maintenance and development of the TPVs (Chen et al. 1996; Dell'Osso and Chen 1986; Shen et al. 1986a; Wang 1987). Li et al. (2011) demonstrated that both dynamic effect and associated condensation latent heat are important in the evolution and eastward movement of the vortices. The heating structure has significant effect on the maintenance of the vortices (Li et al. 2011; Zheng et al. 2013; Wu et al. 2013).

The previous researches exhibited the temporal and spatial distributions of the occurrence frequency of the TPVs as well as the dynamic and thermodynamic effects on the TPVs' generation and evolution processes in summer season. In addition, some researches also demonstrated that the convection, precipitation and surface energy balance over the Tibetan Plateau vary in diurnal timescale (Liu et al. 2002; Oku et al. 2007; Xu and Zipser 2011; Luo et al. 2011). However, it is unclear what the features of the occurrence of the TPVs in diurnal variation are, and how the dynamic and thermodynamic factors affect their diurnal variation. In the present study we will investigate the characteristics of the occurrence frequency of the TPVs in diurnal variation, and the dynamic and thermodynamic factors affecting the diurnal variation. In Sect. 2 we describe briefly the data and method used in the present study. The diurnal variation features of the occurrence frequency of the TPVs and associated precipitation are analyzed in Sect. 3. In Sect. 4 we discuss the effects of the large-scale circulations and thermodynamic factors on the diurnal variation of the TPVs. An analysis on the structure of the atmospheric heating field is made in Sect. 5. The summary and discussion are given in Sect. 6.

2 Data and method

In the present study the TPVs are defined according to the method proposed by LG-TPMR (1981). That is, a vortex over the Tibetan Plateau is a low occurring over the Tibetan Plateau with closed isoheight lines or with cyclonic winds at three observation stations at 500 hPa.

The atmospheric data used in this study is the final operational global analyses data (FNL), which is derived from the Global Forecasting System of the National Centers for Environment Prediction (NCEP), and is gridded $1° × 1°$ at a 6-h interval. The hourly precipitation dataset from the China Meteorological Administration (CMA) is also used. These data cover the period from May to September in 2006–2008.

We also utilize the observational radiosonde data over the Tibetan Plateau at a 12-h interval, and the surface sensible heat from the hourly surface climatic elements
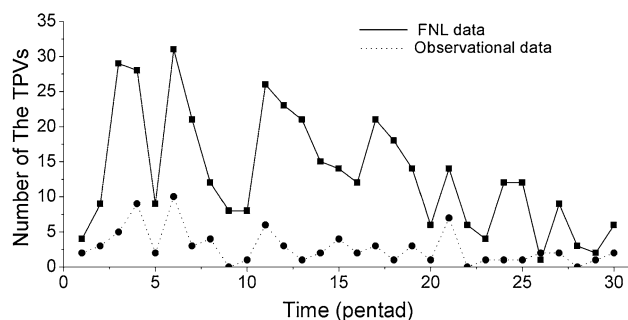
Fig. 1 Variations of the numbers of the TPVs from the FNL data (*solid line*) and observational radiosonde data (*dashed line*) from May to September of 2008

dataset, which are all derived from CMA. Besides, the atmosphere precipitable water vapor (PWV) and the radiosonde data at a 6-h interval provided by JICA/Tibet project (Zhang et al. 2012) are also applied in the present study. These observational data cover the period from May to September in 2008.

The local time (LT) is used in the present study. The observational radiosonde data of twice a day (06 LT and 18 LT) is not enough to exhibit the features of the diurnal variation. In order to check the availability of the FNL data in representing the TPVs over the Tibetan Plateau, we compare the number of the TPVs from May to September in 2008 obtained by the observational radiosonde data and by the FNL data, respectively. As shown in Fig. 1, the number of the TPVs from FNL data is much more than those from the observational data, implying that the FNL data with shorter time interval of 6-h captures more TPVs than the observational data with longer time interval of 12-h. Moreover, similar variations of the numbers from the FNL and observational data can be observed. The correlation coefficient between them is 0.71, which is statistically significant exceeding the 99 % level. Here we can see that the FNL data can basically reflect the variation of the occurrence of the TPVs, and thus is employed in this study.

In our study, the numbers of the TPVs appearing at 06, 12, 18, and 00 LT are considered to be those generated in 00–06 LT, 06–12 LT, 12–18 LT, and 18–00 LT, respectively. We take 78°E–103°E to be the zonal scope of the Tibetan Plateau, in which the spans of 78°E–86°E, 86°E–94°E, and 94°E–103°E are considered as the western, central, and eastern plateau, respectively.

We calculate the atmospheric apparent heat source (Q_1) and apparent moisture sink (Q_2) based on the thermodynamic equation and moisture equation, respectively. The equations used are as follows (Yanai et al. 1973):

$$Q_1 = c_p \left(\frac{\partial T}{\partial t} + V \bullet \nabla T + \omega \left(\frac{p}{p_0} \right)^{\kappa} \frac{\partial \theta}{\partial p} \right), \qquad (1)$$

$$Q_2 = -L\left(\frac{\partial q}{\partial t} + V \bullet \nabla q + \omega \frac{\partial q}{\partial p}\right), \qquad (2)$$

where T is the temperature, V and ω denote the horizontal wind component and the vertical wind component in pressure coordinates, respectively. p_0 is the pressure of 1,000 hPa. c_p represents the specific heat at constant pressure. Its value is 1,004 J Kg^{-1} K^{-1}, and $\kappa \approx 0.286$. θ is the potential temperature. L denotes the latent heat of condensation, and q is the specific humidity. The vertically integrated forms of Eqs. (1) and (2) can be written as follows (Yanai et al. 1973):

$$<Q_1> \approx LP + S + <Q_R> \qquad (3)$$

$$<Q_2> \approx L(P - E) \qquad (4)$$

Here, $<Q_1>$ and $<Q_2>$ are vertically integrated Q_1 and Q_2, respectively. P, S, and E represent the amount of precipitation, surface sensible heat flux, and eddy moisture flux, respectively, and $<Q_R>$ denotes radiative heating (cooling).

3 Spatial and temporal features of the TPVs in diurnal variation

Figure 2 shows the spatial distribution of the TPVs numbers over the Tibetan Plateau appearing at 06, 12, 18, and 00 LT, respectively, based on the statistics in the period from May to September of 2006–2008. In general, most of the TPVs occur over the central-western plateau, and only a few vortices over the eastern plateau. The occurrence of the TPVs reaches the maximum (243 TPVs in total) from evening to midnight (18–00 LT) (Fig. 2d) with the high frequency area in 32°N–36°N, 80°E–92°E. The minimum of the occurrence (54 TPVs in total) is found from early morning to noon (06–12 LT) (Fig. 2b), with a sparse and almost even distribution over the Tibetan Plateau. The numbers of the TPVs appearing in 00–06 LT (Fig. 2a) and 12–18 LT (Fig. 2c) are between the maximum in 18–00 LT and the minimum in 06–12 LT, with 109 and 105 TPVs in total, respectively.

In order to investigate the diurnal variation of the rainfall over the Tibetan Plateau, we calculated the climatological hourly precipitation in a day. In Fig. 3 we show the diurnal variation of the precipitation averaged over the area 32°N–36°N, 80°E–102°E over the Tibetan Plateau, in which, as seen in Fig. 2, most of the occurrence locations of the TPVs are included. The rainfall amount has the minimum at about 10 LT, then increases until reaches the peak period in 18 LT–21 LT, and decreases later on. The diurnal variation of rainfall coincides well with that of occurrence of the TPVs. The minimum occurrence of the
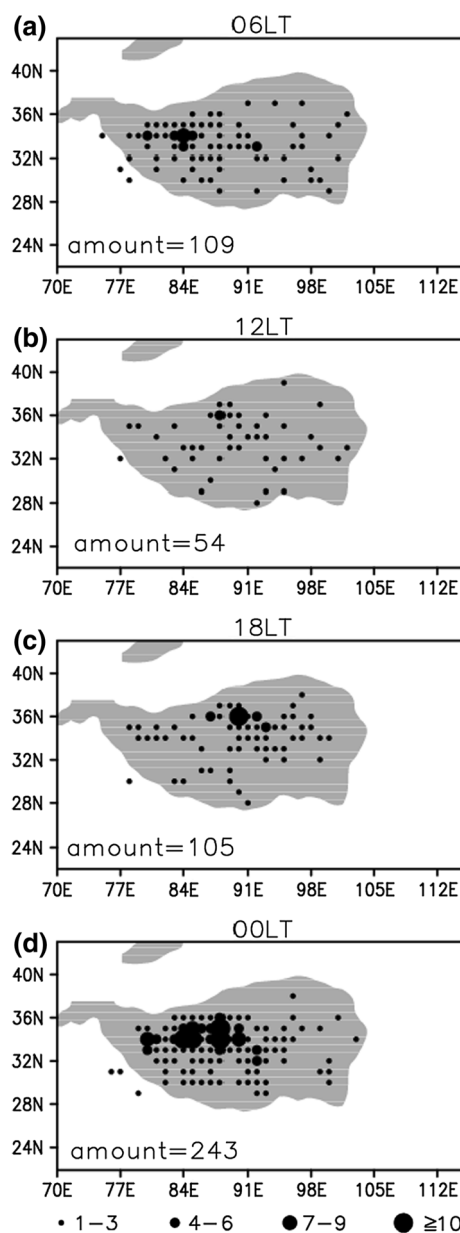
Fig. 2 Spatial distribution of the TPVs' number appearing at **a** 06 LT, **b** 12 LT, **c** 18 LT, and **d** 00LT in the period from May to September of 2006–2008. The size of the *dark spot* denotes the number of the TPVs appearing at the same location, and the shading is the Tibetan Plateau with altitude higher than 3,000 m

TPVs in 06–12 LT (Fig. 2b) corresponds to the valley of the precipitation amount in the same period, while the maximum occurrence of the TPVs in 18–00 LT (Fig. 2d) to the peak period of the precipitation amount. Hence, the diurnal variation of rainfall over the Tibetan Plateau has close relationship with that of the occurrence frequency of the TPVs. More TPVs result in more rainfall, and vice versa.
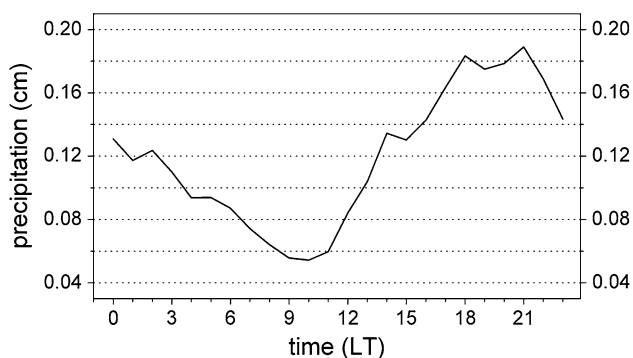
Fig. 3 Diurnal variation of precipitation averaged over the area 32°N–36°N, 80°E–102°E over the Tibetan Plateau (units: cm)

4 Atmospheric dynamic and thermodynamic features in diurnal variation

4.1 Atmospheric dynamic features

Figure 4 shows the composites of the anomalous divergence and winds at 500 hPa in diurnal variation. The anomalies are computed based on the daily mean. At 18 LT (Fig. 4c), there are distinct anomalous northwesterly winds over the western plateau and anomalous northerly winds over the northern plateau. Strong convergence exists over central-western plateau in the area 30°N–36°N, 78°E–93°E, which corresponds well to the high occurrence of the TPVs in 18–00 LT (Fig. 2d). The anomalous convergence at 500 hPa is favorable for the TPVs to generate from evening to midnight (18–00 LT) over the central-western plateau. The large-scale circulations at the other three times are obviously different from those at 18 LT. At 12 LT (Fig. 4b), there are strong anomalous southerly winds over the northwestern plateau and weak westerly winds over eastern plateau, while at 00 LT (Fig. 4d), the anomalous easterly winds are found over the plateau, while anomalous northerly winds exist to the west of 90°E over the northern plateau. There is no apparent convergence at either 12 or 00 LT, resulting in less number of the TPVs appears in 12–18 LT (Fig. 2c) or in 00–06 LT (Fig. 2a). At 06 LT (Fig. 4a), there are anomalous southerly winds over the northern plateau, easterly winds over western plateau, and westerly winds over eastern plateau. The divergent anomalies can be clearly seen over central-eastern plateau, which is accompanied by the smallest occurrence number of the TPVs in 06–12 LT (Fig. 2b). Therefore, the anomalous circulation at 500 hPa at 18 LT is most favorable for the formation of the TPVs from evening to midnight (18–00 LT) and that at 06 LT is most unfavorable from early morning to noon (06–12 LT).

In summertime, the Tibetan Plateau is occupied by the South Asia High and a westerly jet stream exists to the north of the plateau in upper troposphere at 200 hPa (Liu

et al. 2007; Wei et al. 2013), and the jet stream is conducive to the divergence on the right-hand side of its entrance region where the Tibetan Plateau is located. Figure 5 shows the composites of anomalous wind vectors, divergence, and geopotential heights at 200 hPa in diurnal variation. At 18 LT (Fig. 5c), anomalous divergence is found over the plateau. The westerly anomalies to the north of the plateau imply a stronger westerly jet stream, which is favorable for the enhancement of the divergence over the Tibetan Plateau and the positive anomalies of geopotential heights are observed, indicating a stronger South Asia High benefiting divergence at 200 hPa. The easterly anomalies over the plateau and to its north at 12 LT (Fig. 5b) and the weaker westerly anomalies to the north of the plateau at 00 LT (Fig. 5d) correspond well to the weaker positive geopotential heights over the plateau, and result in weaker divergence over the Tibetan Plateau. However, at 06 LT (Fig. 5a) the strong northwesterly anomalies to the north of the plateau reduce greatly the divergence on the right-hand side of the entrance region of the jet stream, and negative anomalies of geopotential heights and convergence anomalies are over the Tibetan Plateau.

Figure 6 shows the height-longitudinal cross-sections of divergence and vertical circulation averaged in 32°N–36°N in diurnal variations. At 18 LT (Fig. 6c), there are divergence anomalies over about 400 hPa and convergence anomalies below, which strengthen the updrafts over the plateau, resulting in more TPVs over the Tibetan Plateau in 18–00 LT. At 06 LT (Fig. 6a), the reduced divergence in upper lever and convergence in lower level lead to anomalous downdrafts over the Tibetan Plateau, resulting in the smallest number of the TPVs' occurrence in 06–12 LT. At both 12 LT (Fig. 6b) and 00 LT (Fig. 6d), over the plateau the divergence anomalies are much weaker and less TPVs appear in both 12–18 LT and 00–06 LT.

Here we demonstrate that the occurrence of the TPVs in diurnal variation can be affected by the diurnal variation of the 200 hPa circulations. The divergence anomalies on the right-hand side of the entrance region of the westerly jet stream directly influence the vertical motion below the South Asia High. The 200-hPa circulations are most beneficial to the TPVs to form from evening to midnight (18–00 LT), and most unbeneficial from early morning to noon (06–12 LT). Considering the strongest 500 hPa convergence anomalies at 18 LT and the weakest at 06 LT, the strongest (weakest) anomalies of ascending motion at 18 LT (06 LT) are (is not) favorable for the TPVs' formation in 18–00 LT (in 06–12 LT).

4.2 Atmospheric thermodynamic features

Figure 7 shows the diurnal variations of the net water vapor transported through the four boundaries of the

Fig. 4 Anomalous divergence (*shadings*; units: 10^{-5} s^{-1}) and winds (*vectors*; units: m s^{-1}) at 500 hPa at **a** 06 LT, **b** 12 LT, **c** 18 LT, and **d** 00 LT. The *red solid lines* are the topographic contours of 3,000 m
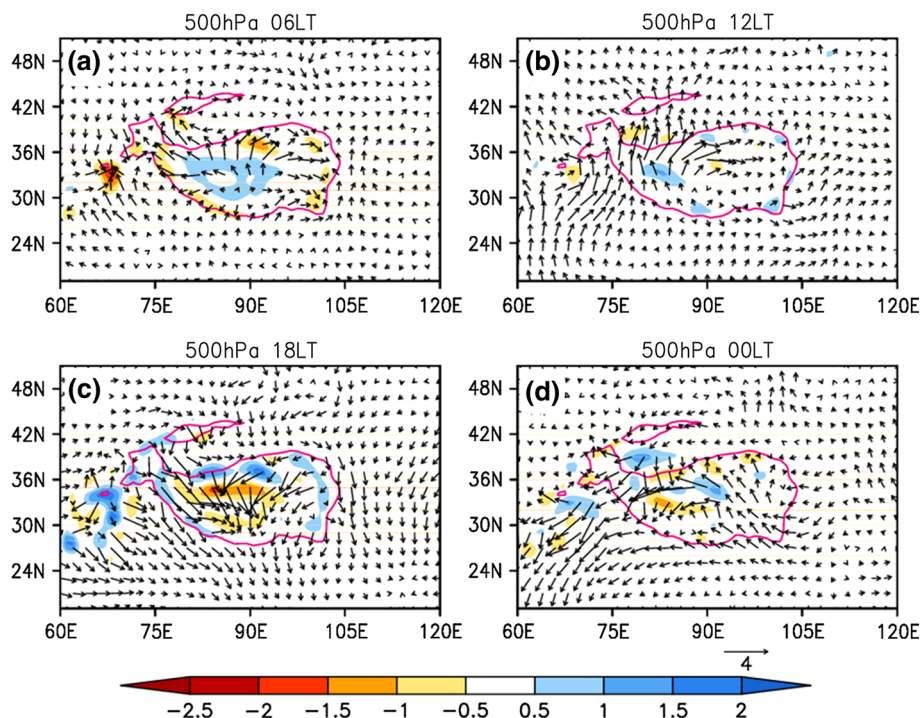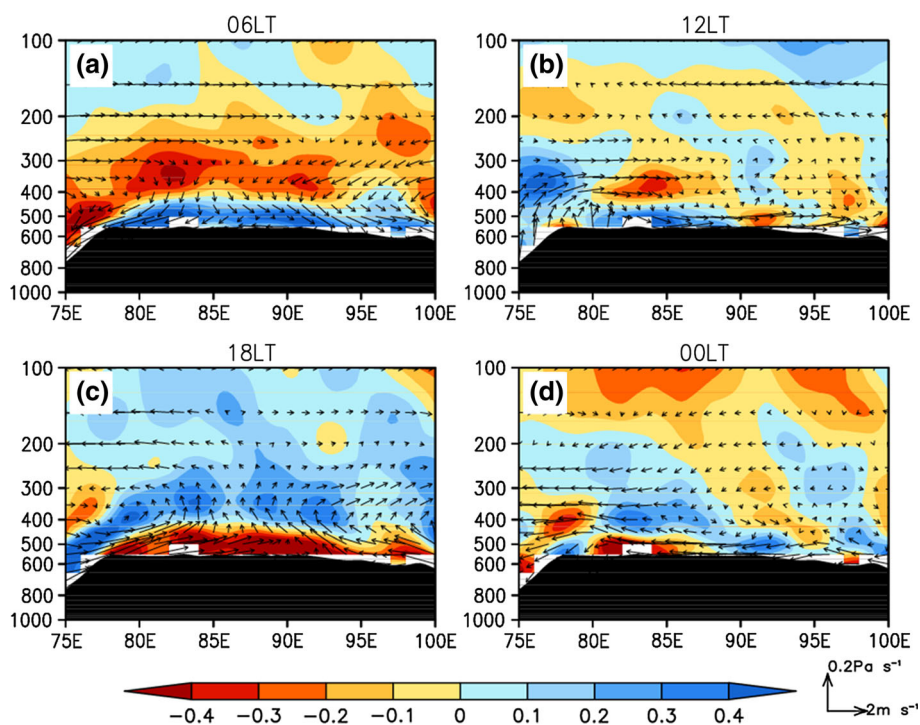
Fig. 5 Same as Fig. 4 but at 200 hPa. The *black contours* denote the geopotential height anomalies (unit: gpm)
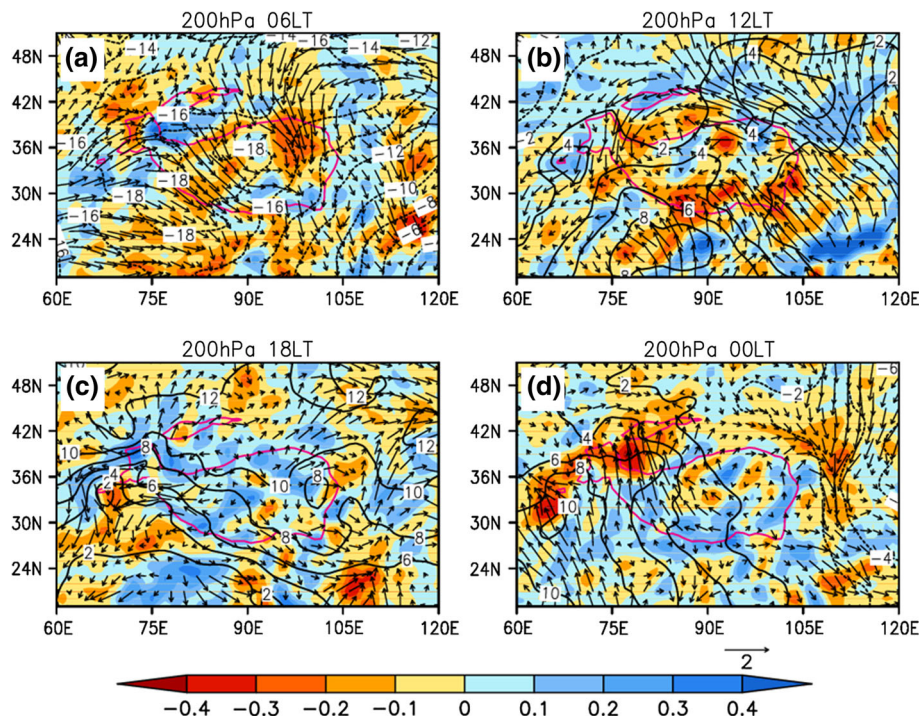
Tibetan Plateau as well as their total net budgets over the Tibetan Plateau. It can be seen that the water vapor flows to the plateau through the south boundary and out of the plateau through east boundary in the whole day. At 06 LT (Fig. 7a) and 00 LT (Fig. 7d), the water vapor is transported out of the plateau through the north boundary, while at 12 LT (Fig. 7b) and 18 LT (Fig. 7c), into the plateau. Besides, through the west boundary there is net water vapor inflow at 06 LT, 12 LT, and 18 LT, but outflow at 00 LT. The water vapor transported from west and north boundaries at 18 LT is much larger than those at other times, and the net inflow of the water vapor to the Tibetan Plateau is

largest with the value being 10.0×10^7 kg s^{-1}, indicating the importance of strong northwesterly winds over the western plateau and northernly winds over the northern plateau (Fig. 4c) in the water vapor transport and highest occurrence of the TPVs in 18–00 LT. In fact, Li et al. (2011) found that the northwesterly winds at 500 hPa invading into the plateau are crucial in generation and maintenance of the plateau vortex. The results here also demonstrate that they are important in highest occurrence of the TPVs in diurnal variation. At 06 LT, the net water vapor supply is smallest with the value being 1.3×10^7 kg s^{-1}, which coincides with the lowest occurrence of the TPVs in 06–12 LT. The net water vapor supplies are 8.0×10^7 kg s^{-1} at 12 LT and 4.5×10^7 kg s^{-1} at 00 LT, respectively, which are smaller than that at 18 LT and larger than that at 06 LT. Consequently, the occurrence number of the TPVs either in 12–18 LT or in 00–06 LT is smaller than that in 18–00 LT and larger than that in 06–12 LT. Here we can infer that the water vapor budget may have close relationship with the occurrence frequency of the TPVs. More (less) water vapor transported to the Tibetan Plateau can lead to more (less) TPVs.

Figure 8 shows the diurnal variation of the atmosphere precipitable water vapor (PWV) and surface sensible heating (SH) observed at seven meteorological stations. Among these stations over the Tibetan Plateau, Gaize (32°18′N, 84°4′E) is located in the western plateau; Dingri (28°39′N, 87°7′E), Naqu (31°29′N, 92°4′E), Longzi (28°25′N, 92°28′E), and Linzhi (29°39′N, 94°22′E) in the

central plateau; and Ganzi (31°37′N, 100°E) and Litang (30°N, 100°16′E) in the eastern plateau. The locations of these stations can be found in Fig. 1a in the paper by Zhang et al. (2012). The characteristics of PWV in diurnal variation observed by these seven stations are similar (Fig. 8a). From evening to midnight (18–00 LT), the PWV keeps at a high level at all stations and the peaks are found in this period, which is consistent with the largest net inflow of the water vapor to the Tibetan Plateau shown in Fig. 7c. Meanwhile, the SH is near zero at this stage (Fig. 8b), which is similar to the results of Chen et al. (2010). From early morning to noon (06–12 LT), the PWV is at the lowest level and its valley exists in the period. Simultaneously, the SH increases gradually and reaches the peak at noon (12 LT), then decreases after 12 LT. Same as the net water vapor flux as shown in Fig. 7, the PWV's peak and valley correspond well to the highest occurrence frequency of the TPVs from evening to midnight (18–00 LT) and the lowest from early morning to noon (06–12 LT), respectively. However, when the SH reaches the peak the occurrence frequency of the TPVs is the lowest, and when the SH is near zero the highest occurrence appears. Therefore, the SH is not the key factor affecting the occurrence of the TPVs, while the sufficient water vapor should have direct effect on the TPVs' formation.

In the JICA/Tibet project (Zhang et al. 2012), the intensive observation in sounding at a 6-h interval was performed at Gaize station located in western plateau. In order to investigate the diurnal variation of the atmospheric stratification status, we use the 6-hourly sounding data

Fig. 7 Water vapor transported through the four boundaries of the Tibetan Plateau and their net budget over the Tibetan Plateau in the area 28°N–37°N, 78°E–103°E at **a** 06 LT, **b** 12 LT, **c** 18 LT, and **d** 00 LT (units: 10^7 kg s^{-1}; *Shadings* indicate the area with altitude exceeding 3,000 m)
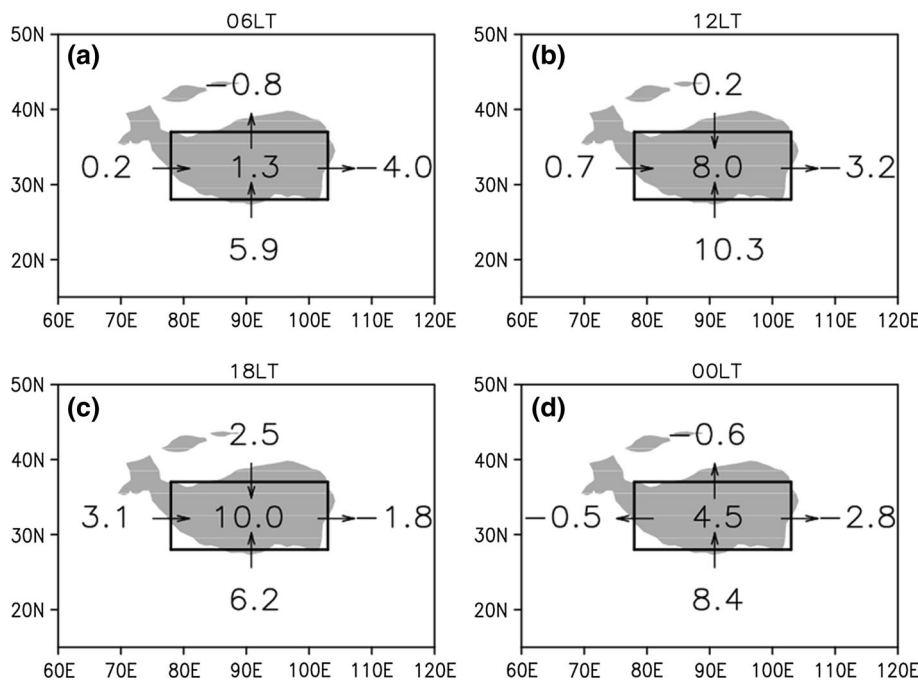
Fig. 8 Diurnal variations of **a** atmosphere precipitable water vapor (PWV) (units: cm) and **b** surface sensible heating (SH) (units: w m^2) observed at seven meteorological stations over the Tibetan Plateau
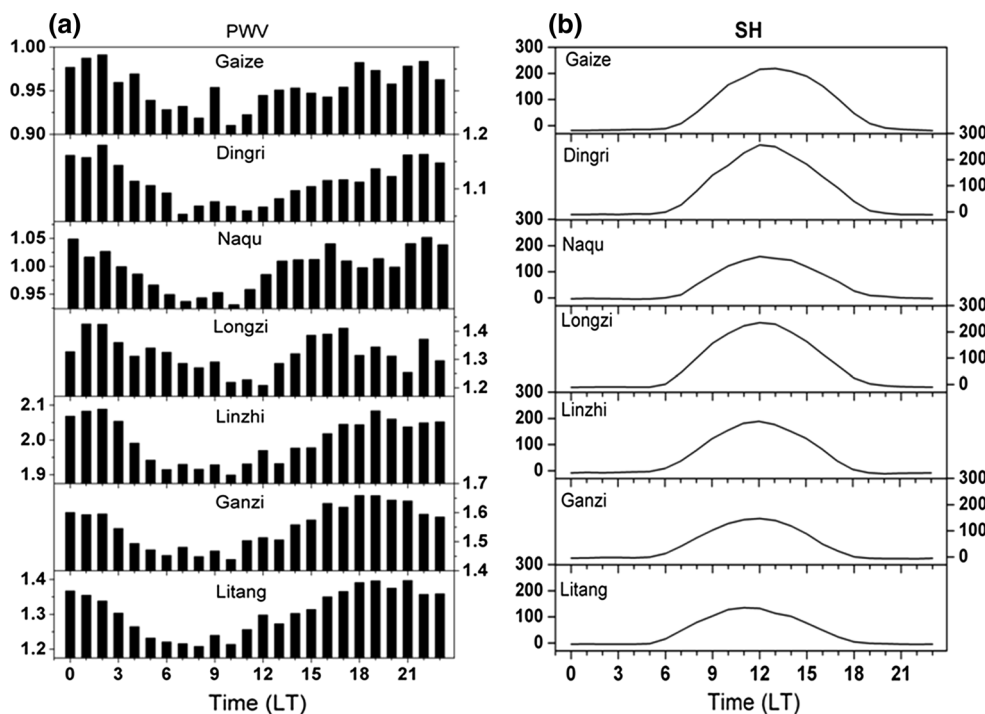
observed at Gaize station to calculate the potential pseudo-equivalent temperature (θ_{se}). The observational times are 23, 05, 11, and 17 LT, respectively. Figure 9 shows the diurnal variation of anomalous θ_{se} profiles. In the period from evening to midnight (17–23 LT), the θ_{se} decreases with altitude but increases from early morning to noon (05–11 LT). Thus, the atmospheric stratifications in 17–23 LT are more unstable compared with those in 05–11 LT.

As seen in Fig. 9, the big differences among the θ_{se} at different times mainly exist in the low level of the atmosphere, indicating that the diurnal variation of water vapor may play an important role in the diurnal variation of the atmospheric stratification instability.

Here we can see that in the evening at 18 LT, there is intensive convergence at 500 hPa, and strong divergence at 200 hPa, which are favorable for the ascending motion
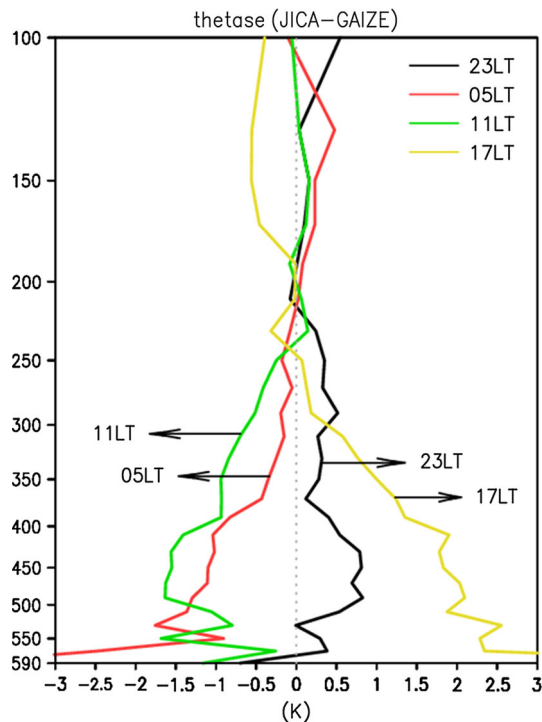
Fig. 9 Profiles of the anomalous potential pseudo-equivalent temperature (θ_{se}) (units: K) at Gaize station (32°18′N, 84°4′E) in western Tibetan Plateau

over the Tibetan Plateau. In addition, the largest amount of water vapor is transported to the Tibetan Plateau and the atmospheric stratification is unstable. The atmospheric conditions at 18 LT obviously are favorable for the water vapor to converge and ascend, leading to the latent heat release. The latent heating depresses the isobaric surface in lower troposphere and strengthens the low-level cyclonic disturbance, which is favorable for the formation of the TPVs in 18–00 LT. On the contrary, the atmospheric conditions in early morning at 06 LT are unfavorable for the occurrence of the TPVs in 06–12 LT.

The maximum sensible heating occurring around 12 LT (Fig. 8b) enhances the convergence over the Tibetan Plateau through the pumping effect (Wu et al. 2007), which exerts direct effect on the TPVs' formation (Li et al. 2011). The enhanced convergence induces abundant water vapor to transport to the plateau, resulting in the accumulation of the instability energy and increase of the stratification instability (Fig. 9). At 6-h time lag around 18 LT, the water vapor transport reaches the maximum (Fig. 7c). Using the water vapor observed by GPS at Lhasa (91.1°E, 29.6°N) in the Tibetan Plateau, Liang et al. (2010) showed the peak of GPS water vapor is about 2 h earlier than the peak times of rainfall frequency and amount. Therefore, the maximum precipitation occurs around 20 LT (Fig. 3).

## 5 Diurnal variation of the atmospheric heating structure

In the previous section we inferred that the latent heat release may have important effect on the formation of the TPVs. In order to further investigate the role of the thermodynamic effects in the occurrence of the TPVs, the diurnal variation of the heating structure over the Tibetan Plateau is investigated in this section.

Figure 10 shows the height-longitudinal cross-sections of diurnal variations in atmospheric apparent heat source (Q_1) and apparent moisture sink (Q_2) averaged between 32°N and 36°N over the Tibetan Plateau. In the early morning at 06 LT (Fig. 10a), both Q_1 and Q_2 are very weak above 500 hPa over the Tibetan Plateau, with positive anomalies of Q_1 and Q_2 mainly near the surface. At noon (12 LT) (Fig. 10b), the heating intensity of Q_1 increases remarkably compared with that at 06 LT, and the heating of Q_1 near the surface reaches the peak of a day because of the largest SH as shown in Fig. 8b. At this time, the maximum of Q_2 appears at 400 hPa near 92°E, and the intensity is a little larger than that at 06 LT. In the evening at 18 LT (Fig. 10c), the Q_2 reaches the peak, and the vertical distributions of Q_1 and Q_2 are quite similar, with their heating centers both in 400–450 hPa between 82°E and 96°E. The consistency of the Q_1 and Q_2 implies that the heating is mainly from the latent heating. As seen in Fig. 3, the rainfall has the peak at 18 LT. Therefore, the latent heat induced by the precipitation is the major component of Q_1 at this time. In fact, the zonal distribution of the TPVs and the largest number of their occurrence from evening to midnight (18–00 LT) (Fig. 2d) are in accordance with the scope and intensity of the latent heating at 18 LT, respectively, indicating that the latent heat has important effect on the formation of the TPVs. At midnight (00 LT) (Fig. 10d), over most parts in the Tibetan Plateau the Q_2 decreases sharply, and its value is evidently smaller than that at 18 LT. The negative Q_1 anomalies appear near surface and in the upper troposphere, respectively, which may result from the radiative cooling at the surface and at the cloud top.

From the analysis above, it is seen that the latent heat reaches maximum in the evening (18 LT) but minimum in the early morning (06 LT), which correspond well to the highest occurrence of the TPVs in 18–00 LT and the lowest occurrence in 06–12 LT. The latent heating can strengthen the low-level cyclonic disturbances through depressing the isobaric surface in lower troposphere, which is favorable for the formation of the TPVs in 18–00 LT. By diagnosing a potential vorticity (PV) equation, Li et al. (2011) demonstrated that the latent heating with its largest center around 400–450 hPa can give rise to a positive PV tendency at 500 hPa, which strengthens the intensity of the

Fig. 10 Height-longitudinal cross-sections of diurnal variations in the atmospheric apparent heat source (Q_1) (*colored shadings*) and apparent moisture sink (Q_2) (*contours*) averaged between 32°N and 36°N at **a** 06 LT, **b** 12 LT, **c** 18 LT, and **d** 00 LT (units: K d^{-1}; *Black shading* indicates the topography of the Tibetan Plateau)
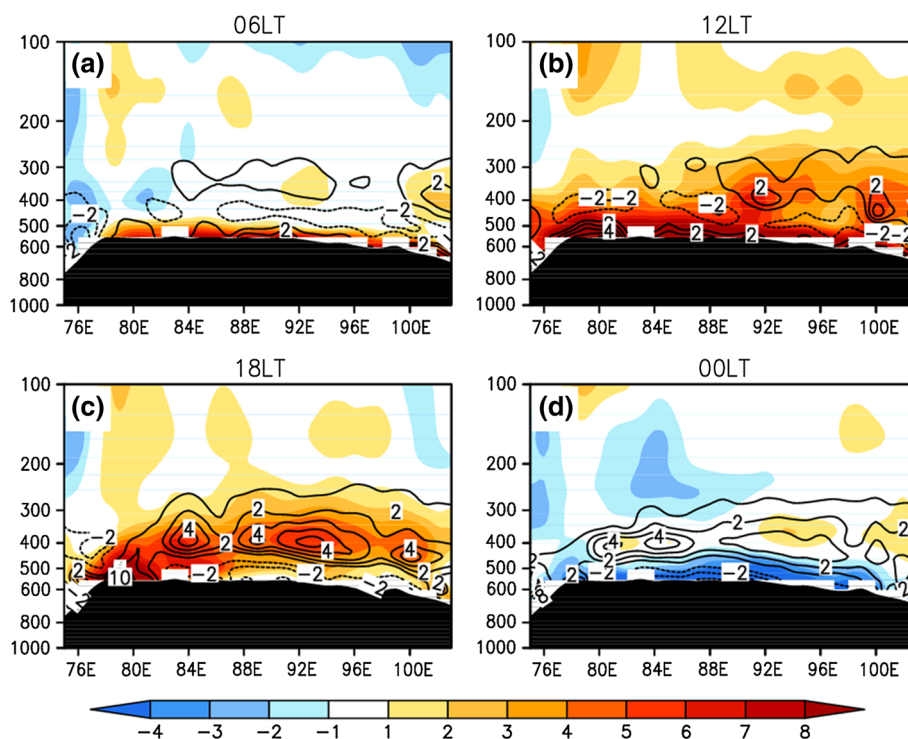
vortex over the Tibetan Plateau. Therefore, the strongest latent heating at 18 LT possibly plays an important role in the largest occurrence number of the TPVs in 18–00 LT.

6 Conclusions and discussions

In this paper we investigated the diurnal variation of the occurrence frequency of the TPVs in the period from May to September of 2006–2008. The dynamic and thermodynamic features in association with the diurnal variation of occurrence frequency of the TPVs are revealed. The main results are as follows:

1. The occurrence frequency of the TPVs shows a robust diurnal variation. It reaches the maximum from evening to midnight (18–00 LT) and minimum from early morning to noon (06–12 LT). The diurnal variation of rainfall over the Tibetan Plateau has close relationship with that of the occurrence frequency of the TPVs. The maximum and minimum occurrences of the TPVs coincide with the peak and valley of the precipitation amount, respectively.

2. Both the anomalous convergence at 500 hPa and divergence at 200 hPa are strongest at 18 LT but weakest at 06 LT, which correspond well to the maximum occurrence of the TPVs from evening to midnight (18–00 LT) and the minimum from early morning to noon (06–12 LT), respectively. The strongest convergence at 500 hPa and divergence at

200 hPa at 18 LT enhance the updrafts and are beneficial to more TPVs to occur over the Tibetan Plateau in 18–00 LT, while the weakest convergence at 500 hPa and divergence at 200 hPa at 06 LT are unfavorable for the ascending motion and in consistency with less formation of the TPVs in 06–12 LT.

3. In the evening (at 18 LT), the strongest water vapor is transported to the Tibetan Plateau and the atmospheric stratification tends to be unstable, which are helpful to give rise to the precipitation and the latent heat release. The largest latent heat appears at 18 LT when the peak of the precipitation occurs. The latent heating depresses the isobaric surface in lower level and forces the low-level cyclonic circulation to generate from evening to midnight (18–00 LT). Therefore, the latent heat induced by the precipitation over the plateau plays an important role in the formation of the TPVs in 18–00 LT.

The previous studies stressed either the dynamic or thermodynamic effects in the formation process of the TPVs. In the thermodynamic effects some researches inferred that the condensation latent heat is the major factor in the PTVs' formation process, while some considered that the surface sensible heat is the key element. Our study points out that both dynamic and thermodynamic effects are important in the generation of the TPVs. The surface sensible heating enhances the convergence over the Tibetan Plateau through the pumping effect (Wu et al. 2007) and is conducive to accumulate the instability energy and

increase the stratification instability. Our study indicates that the formation of the TPVs is accompanied by the co-actions of the large-scale circulations and the latent heat release. Anyway, because the interval of the data used in the present study is 6 h, additional numerical experiments are needed to look into the exact function of the dynamic and thermodynamic effects in the diurnal variation of the TPVs.

References

Chen BM, Qian ZA, Zhang LS (1996) Numerical simulation of formation and development of vortices over the Qinghai-Xizang Plateau in summer. Chin J Atmos Sci 20:491–502 (in Chinese)

Chen Y, Yang K, Zhou D, Qin J, Guo X (2010) Improving Noah land surface model in arid regions with an appropriate parameterization of the thermal roughness length. J Hydrometeorol 11:995–1006

Dell'Osso L, Chen SJ (1986) Numerical experiments on the genesis of vortices over the Qinghai-Xizang Plateau. Tellus 38(A):235–250

LG-TPMR (1981) Research of 500 hPa vortices and shear lines over the Tibetan Plateau in summer. China Science Press, Beijing (in Chinese)

Li GP (2002) The Tibetan Plateau dynamic meteorology. China Meteorological Press, Beijing (in Chinese)

Li GP, Zhao BJ (2002) A dynamical study of the role of surface sensible heating in the structure and intensification of the Tibetan Plateau vortices. Chin J Atmos Sci 26:519–525 (in Chinese)

Li L, Zhang R, Wen M (2011) Diagnostic analysis of the evolution mechanism for a vortex over the Tibetan Plateau in June 2008. Adv Atmos Sci 28:797–808

Liang H, Liu J, Zhang R, Cao Y, Li W (2010) Diurnal variations of atmospheric water vapor in Lhasa river valley. Adv Water Sci 21:335–342 (in Chinese)

Liu L, Feng J, Chu R, Zhou Y (2002) The diurnal variation of precipitation in monsoon season in the Tibetan Plateau. Adv Atmos Sci 19:365–378

Liu Y, Hoskins BJ, Blackburn M (2007) Impact of Tibetan orography and heating on the summer flow over Asia. J Meteorol Soc Japan 85B:1–19

Luo SW (1992) Study on some kinds of weather systems over and around the Qinghai-Xizang Plateau. China Meteorological Press, Beijing, p 205 (in Chinese)

Luo Y, Zhang R, Qian W, Luo Z, Hu X (2011) Intercomparison of deep convection over the Tibetan Plateau-Asian monsoon region and subtropical North America in boreal summer using Cloud-Sat/CALIPSO data. J Clim 24:2164–2177

Oku Y, Ishikawa H, Su ZB (2007) Estimation of land surface heat fluxes over the Tibetan Plateau using GMS data. J Appl Meteorol Climatol 46:183–195

Qiao QM, Zhang YG (1994) Synoptic meteorology of the Tibetan Plateau and its effect on the near areas. China Meteorological Press, Beijing, p 251 (in Chinese)

Shen RJ, Reiter ER, Bresch JF (1986a) Numerical simulation of the development of vortices over the Qinghai-Xizang (Tibet) Plateau. Meteorol Atmos Phys 35:70–95

Shen RJ, Reiter ER, Bresch JF (1986b) Some aspects of the effects of sensible heating on the development of summer weather system over the Qinghai-Xizang Plateau. J Atmos Sci 43:2241–2260

Tao S, Ding Y (1981) Observational evidence of the influence of the Qinghai-Xizang (Tibet) Plateau on the occurrence of heavy rain and severe convective storms in China. Bull Am Meteorol Soc 62:23–30

Wang B (1987) The development mechanism for Tibetan Plateau warm vortices. J Atmos Sci 44:2978–2994

Wei W, Zhang R, Wen M, Rong X, Li T (2013) Impact of Indian summer monsoon on the South Asian High and its influence on summer rainfall over China. Clim Dyn. doi:10.1007/s00382-013-1938-y (in press)

Wu G, Liu Y, Zhang Q, Duan A et al (2007) The influence of mechanical and thermal forcing by the Tibetan Plateau on Asian climate. J Hydrometeorol 8:770–789

Wu G, Zheng Y, Liu Y (2013) Dynamical and thermal problems in vortex development and movement. Part II: generalized slant-wise vorticity development. Acta Meteorol Sinica 27:15–25

Xu WX, Zipser EJ (2011) Diurnal variations of precipitation, deep convection, and lightning over and east of the eastern Tibetan Plateau. J Clim 24:448–465

Yanai M, Steven E, Chu JH (1973) Determination of bulk properties of tropical cloud clusters from large-scale heat and moisture budgets. J Atmos Sci 30:611–627

Yang KM, Bi BG, Li YA, Dong LQ (2001) On flood-causing torrential rainfall in the upstream district of Changjiang River in 1998. Meteorol Mon 27(8):9–14 (in Chinese)

Ye DZ, Gao YX (1979) The Tibetan Plateau meteorology. China Science Press, Beijing (in Chinese)

Yi QJ, Xu XD (2001) The propagation and development of cloud cluster system and severe precipitation event in 1998. Clim Environ Res 6(2):139–145 (in Chinese)

Yu SH (2008) New research advances of the Tibetan Plateau vortex in summer. Torrential Rain Disasters 27(4):367–372 (in Chinese)

Zhang R, Koike T, Xu X, Ma Y, Yang K (2012) A China–Japan cooperative JICA atmospheric observing network over the Tibetan Plateau (JICA/Tibet Project): an overview. J Meteorol Soc Japan 90C:1–16

Zheng Y, Wu G, Liu Y (2013) Dynamical and thermal problems in vortex development and movement. Part I: a PV-Q view. Acta Meteorol Sinica 27:1–14